ScienSage

Journal of Advanced Scientific Research

Available online through https://sciensage.info

ISSN
0976-9595
Research Article

LOW TEMPERATURE COMBUSTION SYNTHESIS AND CHARACTERIZATION OF UN-DOPED AND SAMARIUM DOPED ZINC OXIDE NANOPARTICLES

B.R. Nagabushana[1, 2], M. Vishwas*[3], Daisy Joseph[4], K.V. Arjuna Gowda[5], Satheesh Babu Gandla[6]

[1]*Department of Physics, Sri JCBM College, Sringeri, India*

[2]*Department of Physics, Bharathiar University, Coimbatore, India*

[3]*School of Physics and Geology, Nrupathunga University, Bangalore, India*

[4]*Nuclear Physics Division, Bhabha Atomic Research Centre, Mumbai, India*

[5]*Department of Physics, Government First Grade College, Hoskote, Bangalore, India*

[6]*Interdisciplinary Research Center, R. V. College of Engineering, Bangalore, India*

**Corresponding author: vishwasm46@yahoo.com*

Received: 17-12-2021; Revised & Accepted: 21-04-2022; Published: 31-05-2022

© Creative Commons Attribution-NonCommercial-NoDerivatives 4.0 International License https://doi.org/10.55218/JASR.202213406

ABSTRACT

Zinc oxide (ZnO) and samarium (Sm) doped ZnO nanoparticles (NPs) were synthesised by solution combustion approach using citric acid as fuel. The formation of hexagonal wurtzite structure of pure and Sm doped ZnO powder was prepared and confirmed by x-ray diffraction (XRD). The structure formation, morphological and elemental analysis of pure and Sm doped ZnO powder were analysed using XRD, Raman spectra, scanning electron microscopy (SEM) and x-ray fluorescence spectroscopy (XRF). The results indicated that the trivalent Sm ions were successfully doped in to the lattice of ZnO matrix. The XRD images showed that both ZnO and Sm doped ZnO NPs are highly crystalline, having hexagonal wurtzite structure.

Keywords: ZnO, Samarium, Nanoparticles, Raman spectra, SEM, X-ray diffraction.

1. INTRODUCTION

ZnO is a very popular nano material because of its extensive use in various applications including opto-electronic, technological and industrial domains [1, 2]. In most of the applications, ZnO can replace titanium dioxide (TiO_2) [3-5]. ZnO can be synthesized by various chemical and physical methods [6, 7]. The doping of metal ions plays an important role in improving various properties including optical, electrical, structural, microstructural and chemical properties. Anubhab Sahoo et al. [8] reported the preparation of Mg doped ZnO nanoparticles by pulsed laser ablation technique. They reported the Mg-ZnO as an active material for UV only emission. Othmen et al. [9] reported the fast photo-catalytic degradation of dye under sun light irradiation using Sm doped ZnO nanoparticles prepared by the sol-gel method. The sol-gel method is a cost effective approach for the preparation of metal/semiconductive oxides and perovskite thin films/nanoparticles [10, 11]. They also reported the significant change in photo-luminescence and Raman spectra of Sm doped ZnO nanoparticles. Lathika Devi et al. [12] reported the combustion synthesis and characterization of Sm doped ZnO nanoparticles and showed that the photo-luminescence spectrum of Sm doped ZnO nanoparticles have a strong narrow peak in the blue region at 425 nm with an excitation wavelength of 255 nm.

In this work, the impact of Sm doping on the structural, morphological and elemental variations of ZnO nanoparticles has been investigated.

2. MATERIAL AND METHODS

2.1. Synthesis and characterization of undoped and Sm doped ZnO nanoparticles

The synthesis of ZnO NPs was carried out by solution combustion process. In this process, 4.39 g of AR grade zinc acetate dihydrate ($C_4 H_6 O_4 Zn.2H_2O$) was used as oxidizer and precursor material, 2.1326g of citric acid ($C_6H_8O_7$), as a fuel. An aqueous nitrate solution of Zn was prepared by dissolving zinc acetate dehydrate in dilute nitric acid, the nitrate solution was directly mixed with 2.1326g of citric acid ($C_6H_8O_7$), the mixer was

dissolved in 20ml of double distilled water under continuous stirring.

An additional 10ml dilute nitric acid is added as an energizer. Ammonium Hydroxide is added to the mixture till the pH paper turns orange yellow. The resulting transparent mixture is introduced into the preheated muffle furnace maintained at temperature about 400°C. This exothermic reaction yields white and highly porous ZnO Powder.

The synthesis of 3% samarium doped ZnO ($Zn_{1-x}Sm_xO$ x=0.03) is carried out by solution combustion process. In this process, 4.258 g of AR grade zinc acetate dihydrate used as oxidizer and precursor, 0.1046g of samarium oxide (Sm_2O_3) and 2.1635g of citric acid ($C_6H_8O_7$) as fuel. The process was carried out as mentioned above, finally the exothermic reaction yielded white and highly porous Sm doped ZnO powder.

The crystal structure of ZnO NPs and Sm doped ZnO NPs were determined by x-ray diffractometer with Cu-K_α (1.5405Å) radiation in the scan range 2ɵ between (10-80)° with scan speed of 2°/min and Raman spectrometer. The surface morphology of the sample were estimated by using the SEM (model-JEOL JSM 840A). The x-ray fluorescence (XRF) studies were performed to examine the elemental composition in the samples.

3. RESULTS AND DISCUSSION

The crystal phase and structure of the prepared samples were analysed by x-ray diffraction analysis as shown in Fig. 1. The diffraction peaks and their relative intensities matched with the JCPDS card no. 36-1451, for each sample, all the observed peaks can be indexed as the hexagonal wurzite structure shown in Fig. 2. The average crystallite size of pure ZnO and Sm doped ZnO was calculated using Scherrer's formula [13] and found to be 38nm and 28 nm, respectively. The crystallite size found to be decreased with the doping of Sm.

Fig.3 shows the Raman spectra of pure and Sm doped ZnO nanoparticles. The characteristic Raman peaks observed at 99 cm^{-1} and 436 cm^{-1} are the E_2 (low) and E_2 (high) phonon modes of symmetry, respectively. These peaks confirm the wurtzite phase of ZnO [14]. The observed Raman feature at 327 cm^{-1} is the evidence of second order process (multi-phonon mode) which is the frequency difference between these two strong modes [E_2(H)-E_2(L)]. A_1 and L_1 are the polar modes which further split up into transverse optical (TO) and longitudinal optical (LO) components as observed by Raman features at 377cm^{-1} and 590 cm^{-1}, respectively [15]. The doping of Sm improved the crystallinity and symmetry of ZnO crystals.

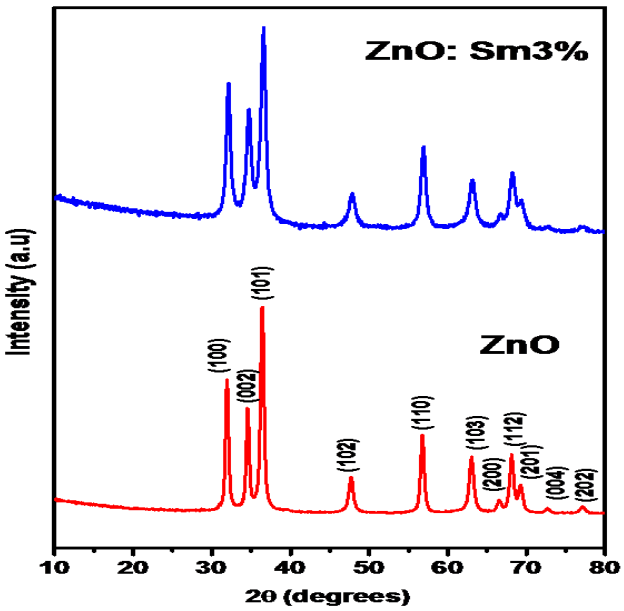


Fig. 1: XRD pattern of ZnO and Sm doped ZnO nanoparticles.

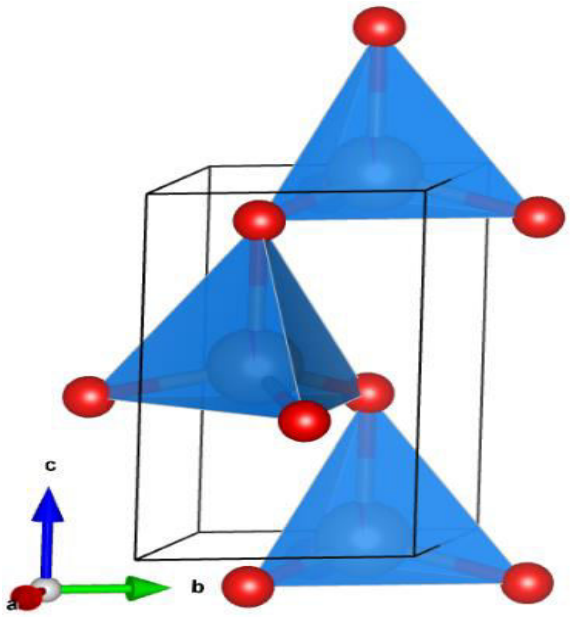


Fig. 2: Crystal structure of ZnO -Wurtzite phase

Fig. 4 shows the SEM images of un-doped and Sm doped ZnO nanoparticles. It can be seen from the figure that, the grains are spherical in shape in both the images and the grain size is of the order of 40-50 nm in un-doped ZnO nanoparticles, while 30 to 45 nm in the Sm doped ZnO nanoparticles. Hence, doping of Sm reduces the

grain size of ZnO nanoparticles. There is slight increase in grain size of nanoparticles compared to XRD results. This is due to the fact that, agglomeration of crystallites can be seen in the SEM images.

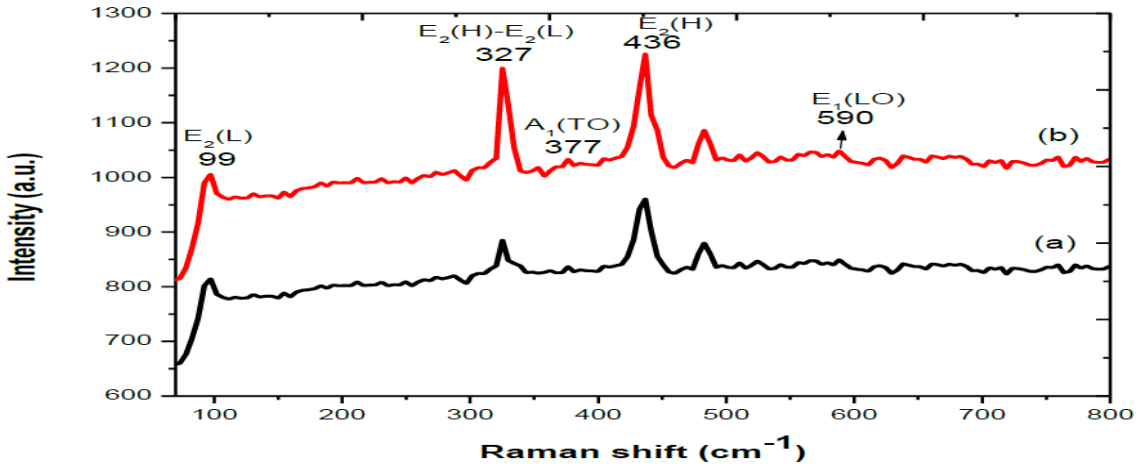


Fig. 3: Raman spectra of un-doped and Sm doped ZnO nanoparticles

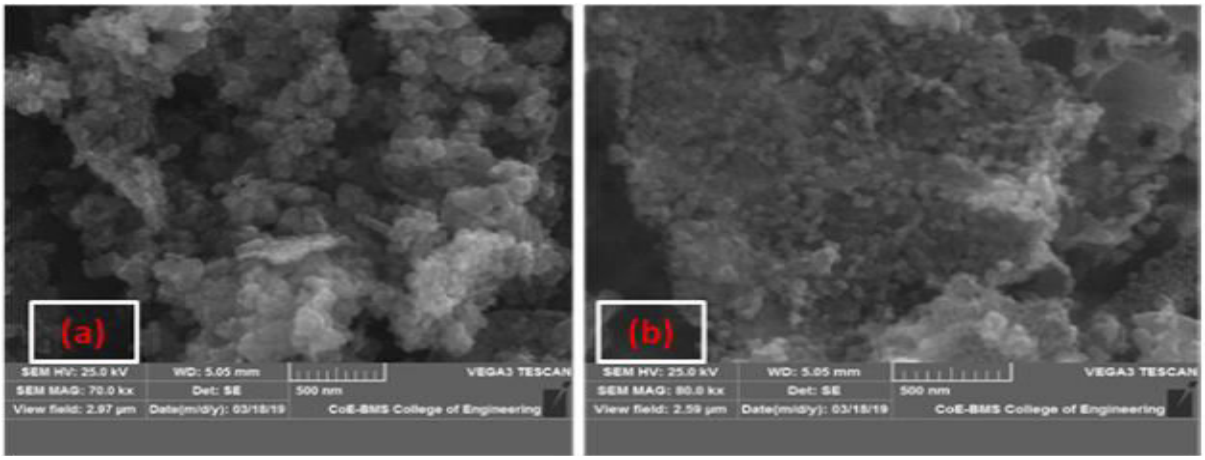


Fig. 4: SEM images of ZnO (a) and Sm doped ZnO (b) nanoparticles

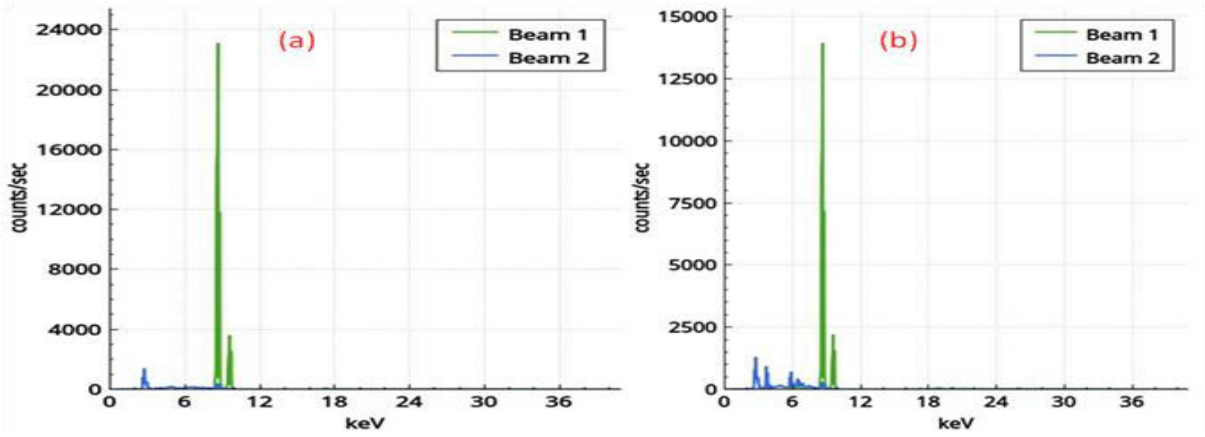


Fig. 5: XRF spectra of ZnO (a) and Sm doped ZnO (b) nanoparticles

Fig. 5 shows the XRF spectra of ZnO and Sm doped ZnO nanoparticles. XRF shows all elements but we are concerned about Zn and Sm. Sm as such is not shown in Table 1, but in spectrum it is the lower energy peak at 5.6 kev which is the Sm L X-ray. In Table 1, Sm is shown as LE. In the pure ZnO, Zn is at 47.2 % which is

shown in spectrum as the green peak at 8.6 KeV. The doping of 3% Sm increases LE from 51.4% to 81.33% and Zn reduces to 16.12%. Ca and Mn also vary drastically with doping. The elemental composition of different elements is also presented in table 1. In the first spectrum of pure ZnO, the prominent peak is shown as blue peak which is Al and green peak which is Zn ka 8.6 KeV and Kb at 9.6 KeV. In the Sm doped ZnO the elements are as follows:

1) Al Ka -1.5 keV
2) Ca Ka-3.6 keV
3) Mn Ka-5.9 keV
4) Fe Ka-6.4 keV
5) Fe Kb-7.00keV
6) Zn Ka-8.6 keV
7) Zn Kb-9.6 keV

Table 1: Elemental analysis of ZnO (a) and Sm doped ZnO (b) nanoparticles

El (a)	PPM	+/- 3σ	El (b)	PPM	+/- 3σ
Al	4500	1800	Al	2200	1200
Si	1010	460	Si	810	340
S	230	160	S	250	100
Ca	802	87	Ca	8510	280
Cr	420	60	Cr	317	50
Mn	275	53	Mn	6240	250
Fe	128	42	Fe	3890	170
Co	146	47	Co	398	50
Ni	334	28	Ni	542	35
Cu	598	67	Cu	206	34
Zn	47.2%	1.8	Zn	16.12%	0.50
Se	146	69	Se	38	20
Rb	191	13	Rb	46	5
Y	235	18	Y	66	8
Zr	661	32	Zr	159	10
Mo	86	56	Mo	33	17
Ba	1560	530	Sn	102	82
Pb	120	32	Ba	960	400
Bi	2470	110	Pb	37	14
LE	51.4%	1.9	Bi	569	36
			LE	81.33%	0.58

4. CONCLUSION

ZnO and Sm doped ZnO nanoparticles are successfully prepared by the solution combustion method. The variation of crystallite size, grain size, zinc concentration and elemental compositions with the doping of Sm, were investigated. XRD and Raman spectra clearly indicated the improvement of crystallinity and symmetry with the doping of Sm in ZnO nano-crystals. The variation of composition (percentage) of ZnO with doping of Sm is clearly understood from XRF results. Hence, the synthesized ZnO:Sm nanoparticles can be used for photo-catalytic and opto-electronic applications.

5. ACKNOWLEDGEMENTS

Authors are grateful to DST for the financial assistance through FIST programme and Central Instrumentation Center, Nrupathunga University, Bangalore.

Conflict of Interest

Authors declare that, there is no conflict of interest for this research.

6. REFERENCES

1. Guo H, Zhou J, Lin Z, *Electrochem Commun*, 2008; **10(1)**:146-150.
2. Kim G, Bang J, Kim Y, Rout SK, Woo SI, *Appl Phys A,* 2009; **97(4)**:821-828.
3. Vishwas M, Sudhir Kumar Sharma, Narasimha Rao K, Mohan S, Arjuna Gowda KV, Chakradhar RPS, *Mod Phys Lett B*, 2010; **24**:807-816.
4. Vishwas M, Narasimha Rao K, Chakradhar RPS, Ashok M. Raichur, *J Mater Sci: Mater Elec*, 2014;**25**:4495-4500.
5. Zeeshan Ali, Bharat Raj, Vishwas M, Anisa Athhar M, *Inter J Curr Microbio &Appl Sci*, 2016; **5(4)**:705-712.
6. Patil SK, Shinde SS, Rajpure KY, *Ceramics International*, 2013; **39(4)**:3901-3907.
7. Li Q, Kumar V, Li Y, Zhang H, Marks TJ, Chang RP, *Chem Mater*, 2005;**17(5)**:1001-1006.
8. Anubhab Sahoo, Miryala M, Dixit T, Klimkowicz A, Francis B, Murakami M, et al. *Nanomaterials*, 2020; **10**:1326-1337.
9. Othmena WBH, Ali MB, W. Bouslama W, Elhouichet H, *Ceramics International, 2020;* **46**:18878-18887.
10. Vishwas M, Narasimha Rao K, Phani AR, Arjuna Gowda KV, Chakradhar RPS, *Spectrochimica Acta Part A*, 2011; **78**:695-699.
11. Vishwas M, Narasimha Rao K, Phani AR, Arjuna Gowda KV, *J Opt*, 2012; **41(1):**60-64.
12. Lathika Devi SK, Sudarsanakumar K, *J Luminescence,* 2010; **130:**1221-1224.
13. Vishwas M, Narasimha Rao K, Arjuna Gowda KV, Chakradhar RPS, *Spectrochimica Acta Part A,* 2010; **77**:330-333.
14. Aurangzeb Khan, *J Pak Mater Soc*, 2010; **4(1)**:5-9.
15. Taziwa R, Ntozakhe L, Meyer E, *J Nanosci Nanotech Res*, 2017; **1(1-3):**1-8.